Virology **296,** 177–189 (2002)
doi:10.1006/viro.2002.1412

The Group-Specific Murine Coronavirus Genes Are Not Essential, but Their Deletion, by Reverse Genetics, Is Attenuating in the Natural Host

Cornelis A. M. de Haan,*[,1] Paul S. Masters,† Xiaolan Shen,† Susan Weiss,‡ and Peter J. M. Rottier*

**Virology Division, Department of Infectious Diseases and Immunology, Faculty of Veterinary Medicine, and Institute of Biomembranes, Utrecht University, 3584 CL Utrecht, The Netherlands; †Wadsworth Center for Laboratories and Research, New York State Department of Health, Albany, New York 12201; and ‡Department of Microbiology, School of Medicine, University of Pennsylvania, Philadelphia, Pennsylvania 19104*

Received December 3, 2001; returned to author for revision January 28, 2002; accepted February 8, 2002

In addition to a characteristic set of essential genes coronaviruses contain several so-called group-specific genes. These genes differ distinctly among the three coronavirus groups and are specific for each group. While the essential genes encode replication and structural functions, hardly anything is known about the products and functions of the group-specific genes. As a first step to elucidate their significance, we deleted the group-specific genes from the group 2 mouse hepatitis virus (MHV) genome via a novel targeted recombination system based on host switching (L. Kuo, G. J.Godeke, M. J. Raamsman, P. S. Masters, and P. J. M. Rottier, 2000, *J. Virol.* 74, 1393–1406). Thus, we obtained recombinant viruses from which the two clusters of group-specific genes were deleted either separately or in combination in a controlled genetic background. As all recombinant deletion mutant viruses appeared to be viable, we conclude that the MHV group-specific genes are nonessential, accessory genes. Importantly, all deletion mutant viruses were attenuated when inoculated into their natural host, the mouse. Therefore, deletion of the coronavirus group-specific genes seems to provide an attractive approach to generate attenuated live coronavirus vaccines.

Key Words: coronavirus; mouse hepatitis virus; reverse genetics; targeted recombination; group-specific genes.

INTRODUCTION

Among the variety of proteins encoded by viruses, those that are responsible for viral replication and virion structure are of primary importance. In addition to these fundamental elements, however, many viruses specify a diverse collection of proteins, the functions of which are often still unclear, but which are known or assumed to be beneficial to the virus. These proteins may either be essential—operationally defined as being required for virus replication in cell culture—or dispensable. Examples include the cytomegalovirus proteins involved in viral immune evasion through the inhibition of MHC class I mediated antigen presentation and the human immunodeficiency virus Vpu and Nef proteins, which downregulate CD4 surface expression (Emerman and Malim, 1998; Ploegh, 1998; and references therein).

Coronaviruses constitute a family of large, positive-sense RNA viruses that usually cause respiratory or intestinal infections in a number of different species, generally in a species-specific fashion. Based on antigenic and genetic criteria, they have been divided into three distinct groups. The feature that all coronaviruses have in common is a characteristic set of essential genes encoding replication and structural functions. Interspersed among these genes are clusters of group-specific open reading frames (ORFs) that are homologous within each group but that differ profoundly among the groups (Lai and Cavanagh, 1997).

Of the common essential genes, the predominant one (ORF 1ab) occupies about two-thirds of the genome. Located at the 5′ end of the genome, this replicase gene encodes two large precursors, the many functional cleavage products of which are collectively responsible for RNA replication and transcription. The other common essential genes specify the four basic structural proteins N, M, E, and S. The nucleocapsid (N) protein packages the viral RNA, forming the core of the virion. This nucleocapsid core structure is surrounded by a lipid envelope in which the membrane (M) protein occurs most abundantly. Associated with the M protein are the small envelope (E) protein and the spike (S) protein, the latter forming the viral peplomers that are involved in virus–cell and cell–cell fusion. The genes for these structural proteins invariably occur in the order 5′-S-E-M-N-3′ and are located in the 3′ third of the viral genome (Lai and Cavanagh, 1997).

In contrast, the identities and the locations of the group-specific genes vary, and their functions have not yet been established (for reviews see Brown and Brierly, 1995; Lai and Cavanagh, 1997; Luytjes, 1995). The vi-

[1] To whom correspondence and reprint requests should be addressed at Virology Division, Department of Infectious Diseases and Immunology, Yalelaan 1, 3584CL Utrecht, the Netherlands. Fax: +31-30-2536723. E-mail: x.haan@vet.uu.nl.

0042-6822/02 $35.00

ruses of group 1, with feline infectious peritonitis virus (FIPV) as probably the most complex member, have as many as three group-specific genes located between the S and E genes and as many as two additional ORFs downstream of the N gene, preceding the 3′-untranslated region of the genome. Group 2 viruses, to which mouse hepatitis virus (MHV) belongs, have two group-specific genes, gene 2a and a hemagglutinin-esterase (HE) ORF between ORF 1b and the S gene. Two additional group 2-specific genes, genes 4 and 5a, reside between the S and E genes. Finally, the group 3 viruses, represented by the prototype infectious bronchitis virus (IBV), have two group-specific genes between the S and E genes as well as two between the M and N genes.

For some strains of MHV, the expression of one or more of the group-specific genes has been demonstrated (Ebner *et al.,* 1988; Yokomori *et al.,* 1991; Zoltick *et al.,* 1990). Indeed, for the best characterized group 2 specific gene product, the HE protein, hemagglutinating and acetyl-esterase enzymatic activities have been demonstrated (Brian *et al.,* 1995). However, in a number of strains or mutants of MHV particular group-specific genes cannot be expressed, either because of failure to transcribe the corresponding mRNA (Luytjes *et al.,* 1988; Yokomori and Lai, 1991) or owing to frameshifting (Weiss *et al.,* 1993) or partial (Schwarz *et al.,* 1990) or complete deletion (Yokomori and Lai, 1991) of an ORF. Thus, many of these genes would appear to be nonessential, at least under certain circumstances. However, this question has never been systematically addressed. To study the functions of the group-specific genes, mutational analyses, including their complete deletion, in a controlled genetic background would be required. The necessary tools to accomplish this have been devised only relatively recently. While for some time a method based on targeted RNA recombination, developed for MHV, was the only such system described (Masters, 1999), other reverse genetic procedures for coronaviruses are now becoming available as well. These procedures use full-length infectious cDNA clones assembled into bacterial vectors (Almazan *et al.,* 2000) or poxviral genomes (Thiel *et al.,* 2001) or assembled *in vitro* (Yount *et al.,* 2000).

As a first step toward elucidating the functions of the coronaviral group-specific genes, we have carried out a deletion analysis of the group 2 virus MHV, strain A59. To this end we established a novel targeted RNA recombination system, which uses switching of host cell tropism as a selection principle for the construction of recombinant viruses. The key tool in this procedure is a recently constructed mutant virus, fMHV, in which the gene segment encoding the spike ectodomain was replaced by that of the FIPV S gene (Kuo *et al.,* 2000). This virus, which grows in feline cells, but not in murine cells, was used as the recombination partner with synthetic RNAs in which the MHV S gene was restored and in which additional intended mutations were engineered. Recombinant viruses were subsequently selected simply on the basis of reacquisition of the ability to grow in murine cells. Our results demonstrated the efficacy of this selection system and showed that the group 2 specific genes, 2a, HE, 4, and 5a, are not essential for viability but that their deletion led to a significant attenuation of MHV in its natural host, the mouse.

RESULTS

Construction of MHV deletion mutants

To examine the role of the group-specific genes of MHV, viruses were prepared from which these genes were deleted by using targeted RNA recombination (Masters, 1999; Masters *et al.,* 1994). The following viral deletion mutants were prepared: MHV-Δ45a, which lacks the ORFs between the S and the E gene; MHV-Δ2aHE, from which the ORFs located between the 1b and the S genes were deleted; and MHV-min, in which both these deletions were combined (Fig. 1). As a control an isogenic wild-type recombinant MHV-A59 (MHV-WT) was reconstructed by the same method used to create the mutants. All viruses were generated by using transcription vector pMH54 (or derivatives thereof) from which defective RNAs were synthesized and composed of the genomic 5′ 467 nucleotides fused to the 3′ end (approximately 8.6 kb) of the genome (Kuo *et al.*, 2000) (Fig. 1). For the removal of ORFs 4a, 4b, and most of 5a, a new junction was generated between the S gene and the E gene (Fig. 1). A small part of the 3′ end of ORF5a, corresponding to a sequence that was preserved in a natural deletion mutant strain of MHV (MHV-S) was maintained (Yokomori and Lai, 1991). This sequence contains the oligopyrimidine tract suggested to be important for initiation of E gene translation (Jendrach *et al.,* 1999). For the deletion of ORFs 2a and HE the transcription vector was extended with the 3′-terminal 1200 bp of the 1b gene, and the 1b sequence was fused to the transcription regulatory sequence [TRS; located at the 5′ end of each gene representing a signal for the synthesis of subgenomic (sg) mRNA (Lai and Cavanagh, 1997; Sawicki and Sawicki, 1998)] that precedes the S gene (Fig. 1). After generation of the transcription vectors, the deletions were recombined into the MHV genome by RNA–RNA recombination with the interspecies chimeric virus fMHV (Fig. 1, top). In this virus the S glycoprotein ectodomain is replaced by that of FIPV, providing this virus with the ability to infect feline cells. By using fMHV as the recipient virus for recombination with donor RNAs carrying the murine S gene, recombinant viruses were easily selected on the basis of their regained natural murine cell tropism (Hsue *et al.,* 2000; Kuo *et al.,* 2000).

Confirmation of the recombinant genotypes

Each recombination experiment yielded viruses that could be propagated on murine cells. The genotypes of

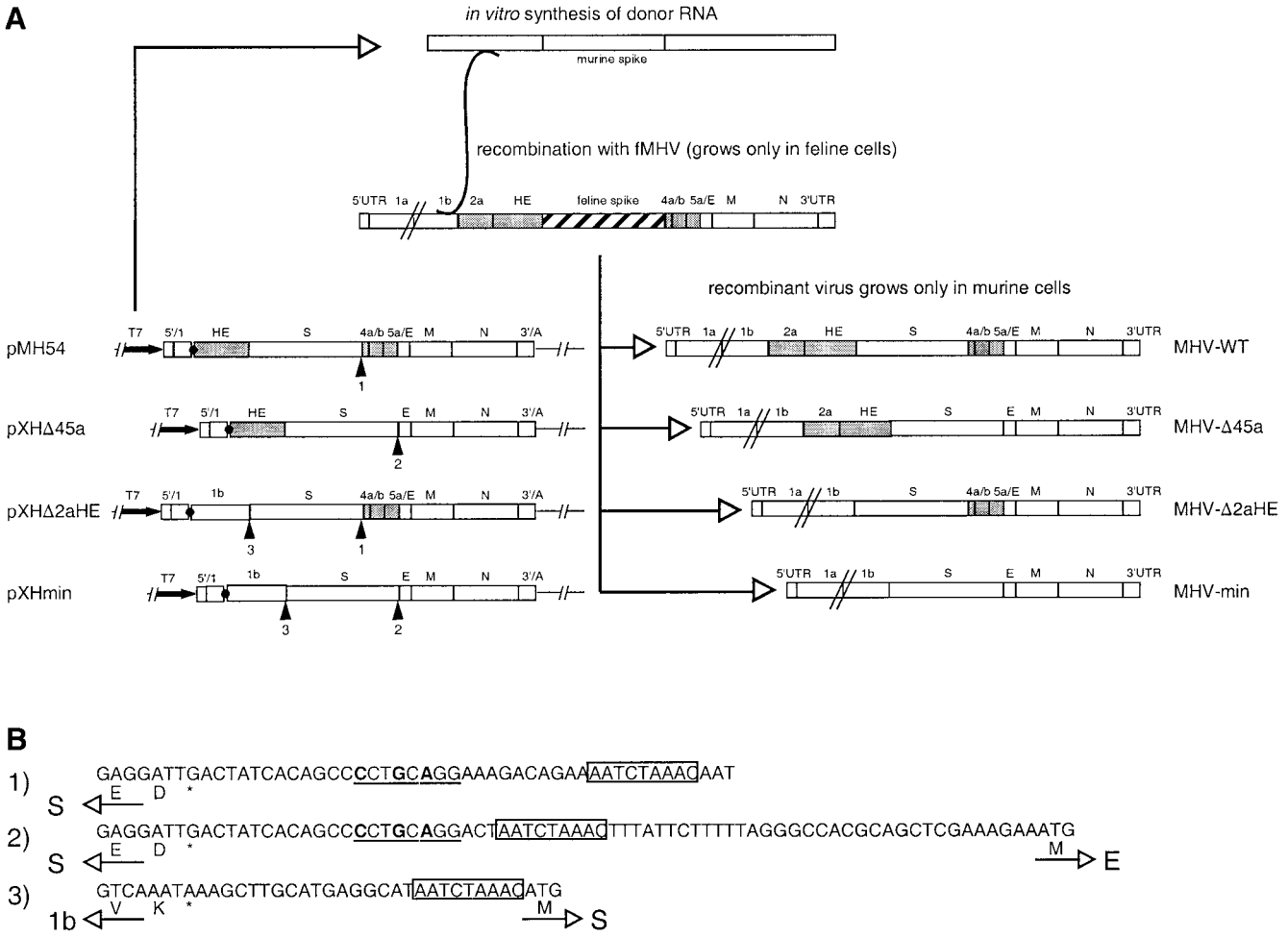

FIG. 1. Plasmid constructs, targeted recombination, and recombinant viruses. (A) The transcription vectors from which the defective RNAs were produced *in vitro* by using T7 RNA replicase are indicated on the left side. Vector pMH54 has been described before (Kuo *et al.,* 2000). The other vectors were derived from pMH54 as described under Materials and Methods. The arrow at the left end of each vector indicates the T7 promoter; the solid circle represents the polylinker between the 5′-end segment of the MHV genome (denoted 5′/1) and either the HE gene or the 3′ end of the replicase gene (1b), followed by the structural and group-specific genes and the 3′-untranslated region and the polyadenylated segment (denoted together as 3′/A). Group 2 specific genes are represented by gray boxes. Positions of the sequences shown in (B) are indicated by arrowheads. On top, a scheme for targeted recombination using the interspecies chimeric virus fMHV, which only grows in feline cells, is shown. The gene encoding the hybrid S protein containing the ectodomain of the feline coronavirus S protein is indicated by a striped box in the fMHV genome. Recombinant viruses generated by the indicated cross-over event can be selected on the basis of their ability to grow in murine cells. The genomes of these viruses are represented on the right side. The 5′- and 3′-untranslated regions are denoted 5′UTR and 3′UTR, respectively. (B) Sequences in the transcription vectors indicated by the arrowheads in (A) are shown and defined as follows: 1, between the S and the 4a gene; 2, between the S and the E gene; and 3, between the 1b and the S gene. The amino acids encoded by the 3′ ends of the S and 1b genes as well as the initiating methionine encoded by the E and S genes are indicated. The MHV TRS is boxed. The *Sse*8387I restriction site downstream of the S gene, created by three nucleotide mutations (bold), is underlined.

the recombinant viruses were confirmed by reverse transcriptase (RT)-PCR performed on genomic RNA, as shown in Fig. 2. To verify the deletion of the ORFs 4 and 5a, the RT step was performed with primer 1092, which is complementary to the 5′ end of the M gene, while the PCR was performed with primers 1261 and 990, which are complementary to the 3′ ends of the E and S genes, respectively. In the case of the MHV-WT recombinant, an RT-PCR product, corresponding in size with the predicted 1328 bp, was observed. As expected, a PCR product of the same length was observed for MHV-Δ2aHE. In contrast, both for MHV-Δ45a and for MHV-min much smaller RT-PCR products were detected, the decrease in size corresponding with the deletion of 736 bp. The deletion of ORFs 2a and HE was analyzed in a similar way. The RT step was performed with primer 1127, which is complementary to the 5′ end of the S gene. The PCR was performed with primers 1173 and 1260, which are complementary to the 3′ end of the 1b gene and the 5′ end of the S gene, respectively. Both for MHV-WT and for MHV-Δ45a the expected PCR products (2409 bp) were detected, which were much bigger than the PCR products detected for MHV-Δ2aHE and MHV-min. The difference in size corresponded with the deletion of 2158 bp.

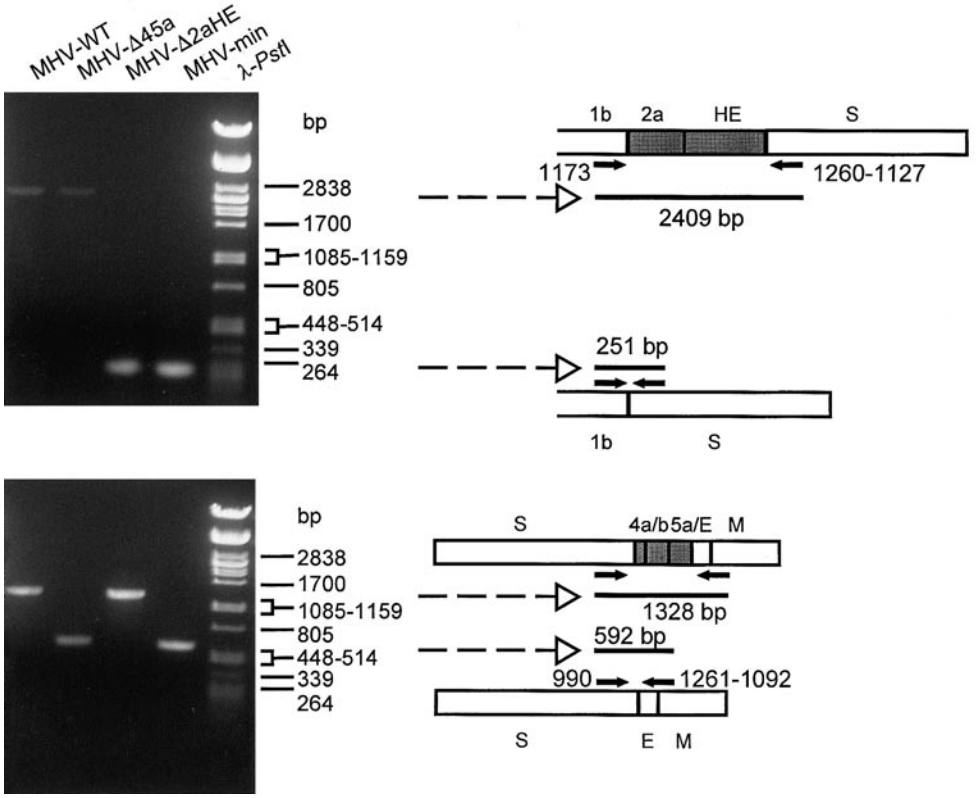

FIG. 2. PCR analysis of MHV recombinants. RT-PCR was used to amplify regions of purified genomic RNA. PCR products were analyzed by electrophoresis in 1% agarose gels stained with ethidium bromide. Sizes of relevant DNA fragments of the marker (λ DNA restricted with *Pst*I) are indicated on the right of each gel. Primers used in each experiment, their approximate loci in the MHV genome, and the predicted sizes of the PCR products are indicated on the right. Primers 1092 and 1127 were used in the RT step, while primer pairs 1261–990 and 1260–1173 were used for the PCR.

Thus, a total of 2894 nucleotides were deleted in MHV-min. Finally, the newly generated junctions, present in the genomes of the deletion mutant viruses (Fig. 1B), were confirmed by sequencing of the RT-PCR products (data not shown). For each virus, pairs of independently generated recombinants were plaque purified and analyzed by RT-PCR. In all cases identical results were obtained. Since the pairs of recombinant viruses grew to very similar titers and the different deletion mutant viruses also serve as independent controls for each other, subsequent experiments were performed with only one independently generated recombinant for each deletion.

RNA synthesis by MHV deletion mutants

To examine the patterns of viral RNA synthesis by the deletion mutants, infected cells were metabolically labeled with [^{33}P]orthophosphate in the presence of actinomycin D. Purified total cellular RNA was analyzed by electrophoretic separation (Fig. 3), and radioactivity in bands of individual viral RNA species was quantitated by phosphorimager scanning (Table 1). For the reconstructed wild-type virus (MHV-WT), the relative molar amounts of the six sg mRNA species and the genomic (g) RNA were similar to those observed previously for MHV (Hsue and Masters, 1999; Jacobs *et al.,* 1981; Leibowitz *et al.,* 1981; Masters *et al.,* 1994) with one notable exception. The 4-5a/E-M-N sgRNA, which is conventionally denoted RNA4, was much more abundant than previously observed for this species in wild-type MHV (Hsue and Masters, 1999; Jacobs *et al.,* 1981; Leibowitz *et al.,* 1981; Masters *et al.,* 1994). The increased synthesis of this particular sgRNA is known to result from three nucleotide changes 13, 15, and 18 bases upstream of the consensus transcription regulatory signal, 5′AAUCUAAAC3′, that precedes gene 4 (Fig. 1B) (X. Shen, L. Kuo, and P. S. Masters, unpublished results; Ontiveros *et al.,* 2001). The three base changes were made in the transcription vector pMH54 to create an *Sse*8387I DNA restriction site downstream of the S gene (Kuo *et al.,* 2000). The reason for the transcriptional upregulation caused by these substitutions is currently unclear.

For the deletion mutants, all variant sgRNAs had mobilities that corresponded to their predicted sizes (Fig. 3 and Table 1), and no prominent extra species were observed. The results of two experiments consistently indicated that the relative molar amounts of the mutant sgRNA species were quite similar to those of their wild-type counterparts, except for a few differences (Fig. 3

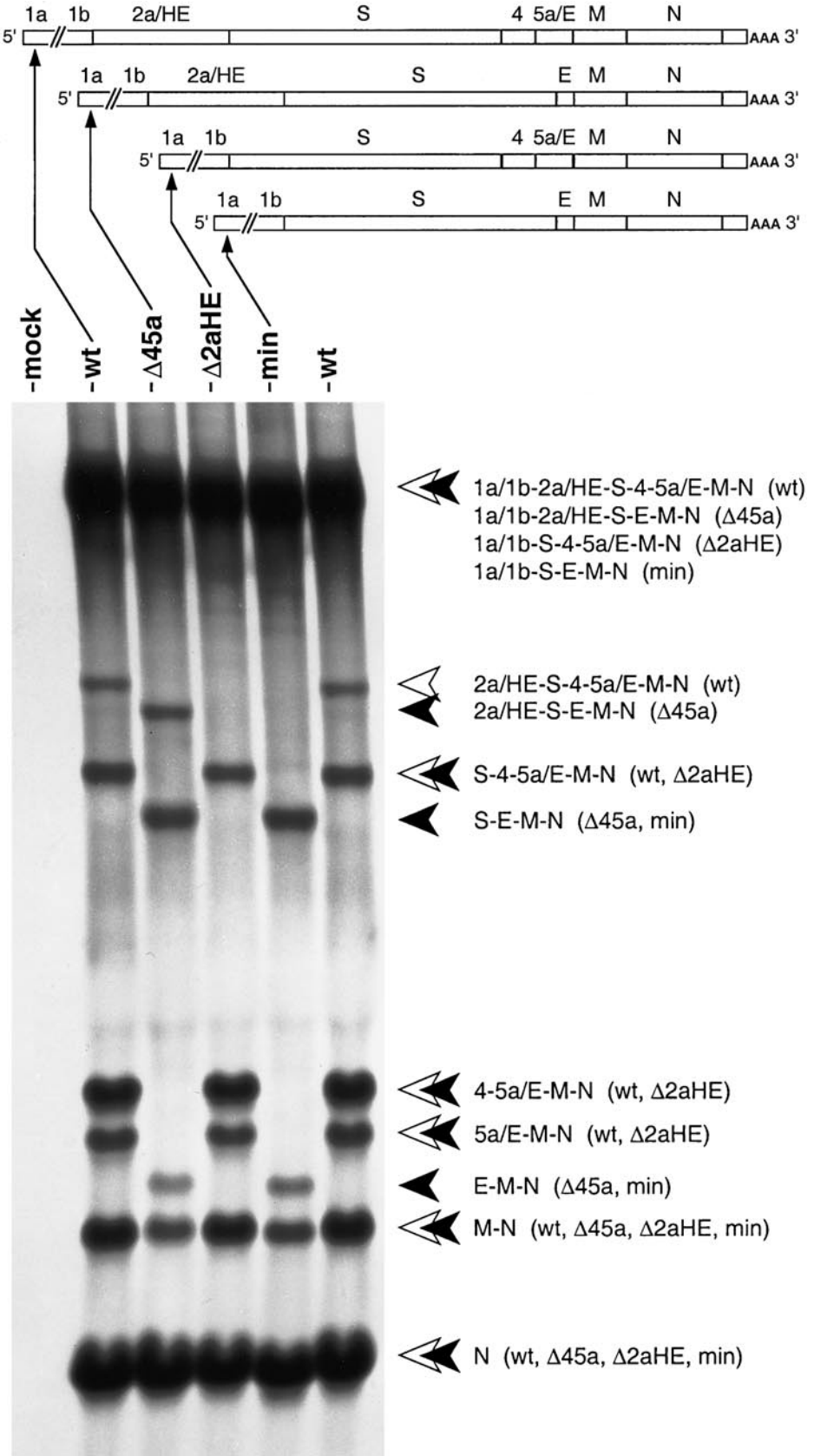

FIG. 3. Analysis of recombinant MHV-induced intracellular RNA synthesis. Mouse 17Cl1 cells were mock-infected or infected with recombinant (WT, Δ45a, Δ2aHE, or min) viruses at a multiplicity of 5 PFU per cell and were labeled with 111 μCi [^{33}P]orthophosphate per ml from 6 to 8 h postinfection in the presence of 20 μg actinomycin D per ml, as described previously (Masters *et al.,* 1994; Hsue and Masters, 1999). Purified total cytoplasmic RNA was separated by electrophoresis through 1% agarose containing formaldehyde, and labeled RNA was visualized by fluorography. The genomic composition of each virus is indicated schematically at the top. Open arrowheads and closed arrowheads, respectively, indicate wild-type and deletion mutant genomic and subgenomic RNA species.

TABLE 1

RNA Synthesis by Recombinant MHVs[a]

Virus[b]	RNA species	RNA length (nt)[c]	Molar ratio[d]
WT(1)	1a/1b-2a/HE-S-4-5a/E-M-N	31,528	1.00
	2a/HE-S-4-5a/E-M-N	9852	0.14
	S-4-5a/E-M-N	7677	0.40
	4-5a/E-M-N	3664	2.13
	5a/E-M-N	3281	1.14
	M-N	2641	3.72
	N	1944	11.95
WT(2)	1a/1b-2a/HE-S-4-5a/E-M-N	31,528	1.00
	2a/HE-S-4-5a/E-M-N	9852	0.15
	S-4-5a/E-M-N	7677	0.42
	4-5a/E-M-N	3664	2.24
	5a/E-M-N	3281	1.24
	M-N	2641	3.45
	N	1944	12.38
Δ45a	1a/1b-2a/HE-S-E-M-N	30,792	1.00
	2a/HE-S-E-M-N	9116	0.29
	S-E-M-N	6941	0.59
	E-M-N	2935	0.67
	M-N	2641	2.03
	N	1944	15.74
Δ2aHE	1a/1b-S-4-5a/E-M-N	29,370	1.00
	S-4-5a/E-M-N	7677	0.71
	4-5a/E-M-N	3664	3.85
	5a/E-M-N	3281	1.59
	M-N	2641	5.11
	N	1944	14.03
min	1a/1b-S-E-M-N	28,634	1.00
	S-E-M-N	6941	0.73
	E-M-N	2935	0.74
	M-N	2641	1.40
	N	1944	14.16

[a] Radioactivity in RNA bands shown in Fig. 3 was quantitated by scanning with Image Quant Phosphorimager.

[b] All viruses are recombinant viruses. WT(1) and WT(2) refer to parallel infections with MHV-WT shown on the left and right side of Fig. 3, respectively.

[c] RNA length includes a poly(A) tail of 200 nucleotides (nt).

[d] Molar ratio ($g = 1$) is normalized with respect to moles of genomic RNA.

and Table 1). First, deletion of the ORF 4/5 cluster reduced the relative molar levels of M-N and E-M-N sgRNAs as compared to their wild-type counterparts. Second, for cells infected with the Δ2aHE mutant, the S-4-5a/E-M-N, 4-5a/E-M-N, 5a/E-M-N, and M-N sgRNAs, but not the N sgRNA, were all relatively overproduced with respect to their recombinant wild-type counterparts. The reasons for these changes are presently unknown, but they may be caused by longer range effects of overall genomic structure on the efficiency of discontinuous transcription at individual TRSs.

Analysis of viral proteins

To analyze the viruses at the protein synthesis level, cells were infected with the different recombinant viruses and labeled for 3 h with ^{35}S-labeled amino acids. The culture media were then collected and cleared by low-speed centrifugation, while the cells were lysed. Subsequently, culture media and cell lysates were processed for immunoprecipitation with several antibodies followed by sodium dodecyl sulfate–polyacrylamide gel electrophoresis (SDS–PAGE) using a 15 or 20% gel. As shown in Fig. 4A (left), S, N, and M proteins could be precipitated from the cell lysates with the polyclonal anti-MHV serum. For the M protein the O-glycosylated M_3 species containing *N*-acetyl-galactosamine, galactose, and sialic acid (Krijnse Locker *et al.,* 1992) was predominant. The radioactivity in each protein was quantitated by phosphorimager scanning of the dried gel to determine the relative amounts of the proteins present in the cells. From the results of three independent experiments, it appeared that the M/N ratio in cells infected with MHV-Δ45a or MHV-min, but not with MHV-Δ2aHE, was significantly reduced as compared to MHV-WT infected cells (Fig. 4B). Significant changes in the S/N ratio were not observed. These results correlate with the relative reduction of M-N sgRNA in MHV-Δ45a and MHV-min infected cells (Table 1).

Because the N protein has been found to be secreted into the culture medium of infected cells also in a non-lipid associated form (Opstelten, 1995), the extracellular quantity of this protein is not a reliable measure of virus assembly. We therefore used the M protein for this purpose and determined the relative amount of radiolabeled protein that is secreted. As Fig. 4A (right) shows, consistently less M protein was immunoprecipitated from the culture media of MHV-Δ45a- and MHV-min-infected cells than of MHV-WT- or MHV-Δ2aHE-infected cells. Quantitation of the results of three independent experiments showed that the relative amounts of the M protein released from MHV-Δ45a- and MHV-min-infected cells—expressed as the ratio of extracellular over cell-bound M protein (M outside/inside)—were decreased by approximately 50% (Fig. 4B), which indicates that less viral particles were produced.

To confirm the deletion of the 2a gene in two of our mutant viruses, we analyzed the cell lysates by immunoprecipitation with a protein 2a specific antiserum (Zoltick *et al.,* 1990) (Fig. 4C). This antiserum is known to nonspecifically immunoprecipitate the N protein which thus served as an internal control. As expected, the 2a protein, with a predicted molecular weight of 31 kDa, was observed (to the same extent) in lysates prepared from cells infected with MHV-WT and with MHV-Δ45a but not from MHV-Δ2aHE- and MHV-min-infected cells.

Finally, the expression of the E gene was analyzed. To our initial surprise, E protein could only be detected in control cells infected with the wild-type MHV-A59 strain from the Utrecht laboratory and not in any of the recombinant virus infected cells (Fig. 4D). Careful analysis of the sequence of the E gene in the Utrecht MHV-A59

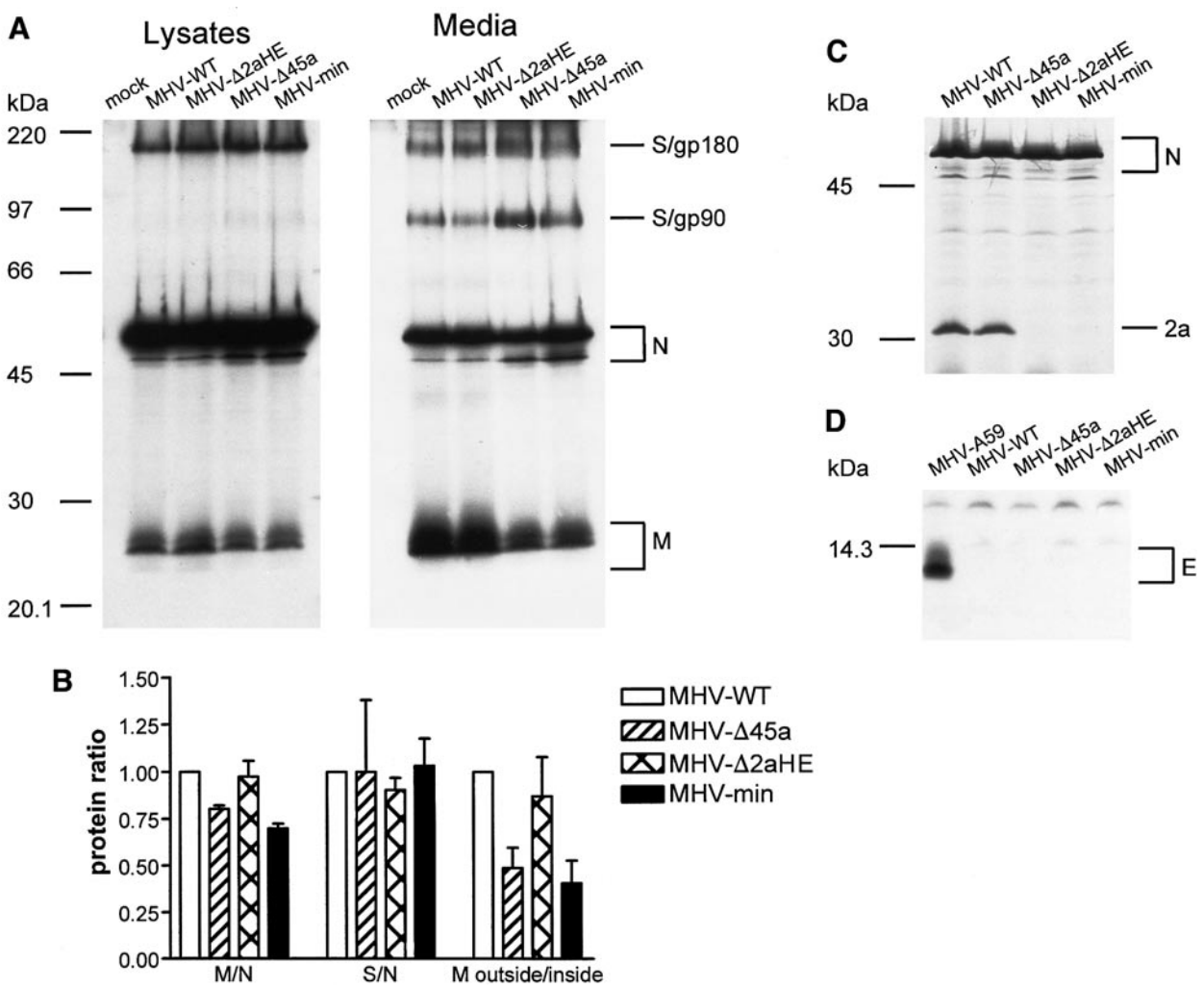

FIG. 4. Analysis of synthesis and release of recombinant MHV proteins. LR7 cells were mock infected or infected with recombinant (WT, Δ45a, Δ2aHE, or min) viruses or with the Utrecht laboratory wild-type virus (MHV-A59) as indicated on the top of each gel. Cells were labeled for 3 h with ^{35}S-labeled amino acids starting 5 h postinfection. (A) Both cells (left) and media (right) were prepared and used for immunoprecipitation with the anti-MHV serum K134, and the precipitates were analyzed by SDS–15% PAGE. (B) For quantitative analysis phosphorimager scanning of the amount of radioactivity in the M, S, and N proteins in the dried gels of three independent experiments (as shown in A) was performed. The ratios of the intracellular amount of M and N (M/N) and S and N (S/N) proteins were calculated relative to MHV-WT infected cells and standard deviations are indicated. The ratio of the amount of M protein present in the culture media and in cells (M outside/inside) was also determined. Cells were also prepared for immunoprecipitation with the anti-2a serum UP3 (C) and with the anti-E serum K5379 (D). The precipitates were analyzed by SDS–15% PAGE and SDS–20% PAGE, respectively. The positions of the different proteins are indicated on the right, while the molecular mass marker is indicated on the left of each gel.

strain revealed that it differs at two nucleotide positions from the E gene in the transcription vector pMH54 (Kuo *et al.*, 2000) (A217G and T230C), which is based on the sequence of the Albany laboratory strain of MHV-A59. These nucleotide changes result in two amino acid substitutions (M73V and L77P). The sequence of the E gene from the Utrecht MHV-A59 is identical to that of MHV-3 (Fischer *et al.,* 1998). Since the anti-E serum was raised against a fusion protein based on the Utrecht MHV-A59 sequence (Raamsman *et al.,* 2000), we considered this difference to be the most likely explanation for the lack of E protein precipitation. Indeed, when we substituted the two nucleotides in the E gene of pMH54, the resulting recombinant virus expressed an E protein that could now be precipitated with our anti-E serum to the same extent as the E protein produced by the Utrecht MHV-A59 (data not shown).

Tissue culture growth phenotype

Next we compared the recombinant viruses for their *in vitro* growth characteristics. No differences were observed with respect to their cytopathic effects. They all induced extensive syncytia to the same extent as the Utrecht wild-type virus, while plaque sizes on LR7 cells were also not appreciably different. Differences were,

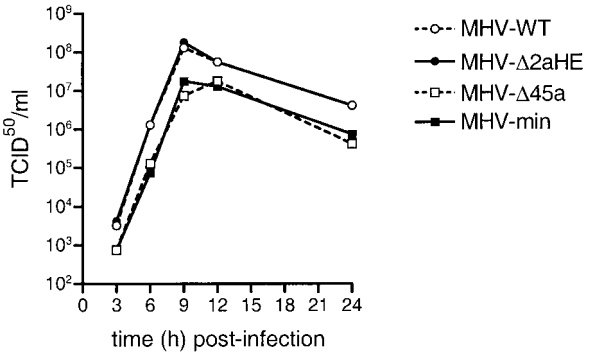

FIG. 5. Single-step growth kinetics of the MHV recombinants. LR7 cells were infected with each recombinant MHV at a multiplicity of 8 PFU per cell. Viral infectivity in culture media at different times postinfection was determined by a quantal assay on LR7 cells, and 50% tissue culture infective doses ($TCID_{50}$) were calculated.

however, observed in their one-step growth curves. Though all viruses displayed similar kinetics, MHV-Δ45a and MHV-min appeared to reach approximately 10-fold lower titers than MHV-WT and MHV-Δ2aHE (Fig. 5), which behaved similar to wild-type MHV-A59 (data not shown). These observations are consistent with the results of the immunoprecipitation assays which showed that, taking the appearance of the M protein as a measure, MHV-Δ45a and MHV-min were less efficiently assembled and released.

Virulence of recombinant viruses

Having analyzed their *in vitro* growth characteristics, the properties of the recombinant viruses were characterized in their natural host, the mouse. Thus, we determined their virulence. Mice were inoculated intracranially with 5- or 10-fold serial dilutions of MHV-WT, MHV-2aHE, MHV-45a, and MHV-min. Infected mice were observed for clinical signs and lethality. For the recombinant wild-type virus a 50% lethal dose (LD_{50}) value of 2.7×10^4 (mean of two experiments) was calculated (Hingley *et al.,* 1994; Reed and Muench, 1938). This LD_{50} value is five to eight times higher than the values that are usually obtained for MHV-A59 lab strains. Although the reason for this difference is not clear, it underscores the importance of taking an isogenic wild-type recombinant virus along. LD_{50} values were not able to be calculated for the three deletion viruses, but must be in excess of 2.5×10^5, the highest concentration inoculated, as none of the mice inoculated with this dose died. Figure 6 illustrates the kinetics of mortality of mice infected with the highest dose inoculated, 2.5×10^5 plaque forming units (PFU), of WT and deletion viruses. While all the animals inoculated with wild-type virus had died by 7 days postinfection, the deletion viruses were highly attenuated, displaying no death and less severe clinical symptoms. Despite the observation of no mortality, all mice infected with the Δ45a and Δ2aHE viruses showed clinical signs of hunched posture, disheveled appearance, and waddling gait during the first week postinfection; these symptoms were less severe and observed in fewer mice infected with MHV-min. Thus, all deletion viruses are attenuated relative to wild-type virus; however, the genetically minimized coronavirus seems attenuated more severely than the other deletion viruses.

DISCUSSION

One of the most distinguishing features of the coronavirus family subgroups is the nature and genomic locations of their group-specific genes. With the exception of the HE gene, essentially nothing is yet known about these genes. We now show for the group 2 coronavirus MHV, using our newly developed strategy of targeted recombination, that these group-specific genes are not essential, since recombinant viruses, from which these group-specific genes were fully deleted, could be easily recovered. While deletion of the 2a/HE gene cluster did not affect growth *in vitro*, deletion of the 4/5a cluster resulted in viruses that replicated to a 10-fold lesser extent. In addition, our work shows that deletion of the nonessential genes led to significant attenuation of all the viruses when inoculated into mice and therefore provides an attractive approach to generate attenuated live coronavirus vaccines.

Except for the HE protein little is known about the actual proteins encoded by the group 2 specific coronavirus genes, and this holds true as well for the group-specific proteins of the other groups. The HE protein is a type I glycoprotein, which forms disulfide linked homodimers (Brian *et al.,* 1995 and references therein). Viruses that express this protein show a second, shorter fringe of peplomers on their virions. For the HE protein hemagglutinating and acetyl-esterase activities have been demonstrated, but the significance of these prop-

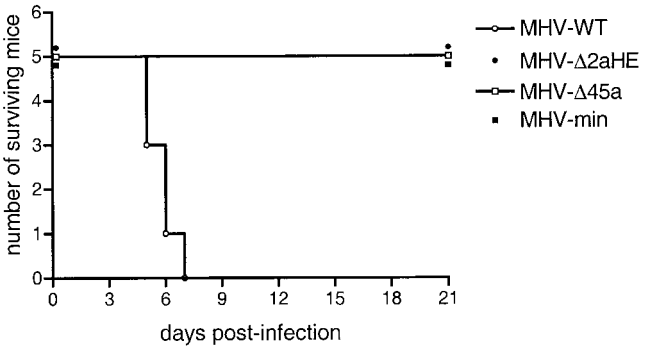

FIG. 6. Survival of C57Bl/6 mice infected with MHV recombinants. Four-week-old mice were inoculated intracranially with various dilutions of recombinant wild-type and deletion viruses ($n = 5$ per virus) and survival was monitored. The data for mice infected with 2.5×10^5 PFU are shown. While the animals infected with MHV-WT had all succumbed by day 7 postinfection, all mice inoculated with the deletion mutant viruses survived until 21 days postinfection.

erties remains to be established. No enzymatic activities have been assigned to the other group-specific proteins. The 31-kDa 2a protein was detected in the cytoplasm of MHV, bovine coronavirus (BCoV), and human coronavirus (HCoV)-OC43 infected cells (Bredenbeek *et al.,* 1990a; Cox *et al.,* 1991; Labonte *et al.,* 1995; Zoltick *et al.,* 1990). The MHV and BCoV 2a proteins share 45% amino acid identity. The BCoV 2a protein was demonstrated to be a phosphoprotein (Cox *et al.,* 1991), but this modification could not be found for MHV (Bredenbeek *et al.,* 1990a). While the MHV 2a protein contains a putative nucleotide binding site (Luytjes *et al.,* 1988), this site is not conserved in the 2a sequence of BCoV and HCoV-OC43. Interestingly, the amino-terminal half of the coronavirus 2a protein has significant sequence identity with the carboxyl-terminal part of the torovirus 1a polyprotein (31–36%) (Snijder *et al.,* 1991), which is presumably involved in viral RNA synthesis. The same 2a protein domain is also homologous with the carboxyl-terminal domain of the group A rotavirus VP3 protein (20–25%), which is part of the virion core and has capping activity (Chen *et al.,* 1999). It cannot be excluded that these proteins have additional, common functions. Very little is known about the (putative) gene 4 and 5a products. The expression product of MHV-JHM (but not of MHV-A59) gene 4 has been demonstrated in infected cells (Ebner *et al.,* 1988; Weiss *et al.,* 1993). This protein is predicted to be an integral membrane protein (Skinner and Siddell, 1985). It has a strikingly high content of threonine residues outside the hydrophobic region. The putative ORF5a expression product has not been demonstrated in infected cells, and it has been proposed that the actual role of this region is to function as an internal ribosome entry site for the translation of the E protein. No homologies have been found for the putative products of ORFs 4 and 5a with other than group 2 coronavirus-specific sequences.

The coronaviral group-specific genes nor their protein products are required for replication at the level of the individual cell. Deletion of the 2a/HE gene cluster was without appreciable effect on *in vitro* viral growth, while viruses lacking the 4/5a cluster reached 10-fold lower titers. Whether this latter effect was at all due to the respective proteins not being produced is unclear. The reduced replication capacity of the Δ4/5a viruses might simply be the consequence of the deletion per se. These viruses exhibited lower transcription efficiencies for the sgRNAs from which the M and E genes are translated. The effect thereof on the synthesis of the E protein could not be analyzed due to the lack of an appropriate antiserum. However, the reduced synthesis of the sgRNA encoding M correlates with the observed slight but significant decrease in the M protein expression level. In view of the essential role of the M and E proteins in viral assembly (Vennema *et al.,* 1996), this may well explain the impaired replication capacity of these viruses. A comparable result was observed for the equine arteritis virus. This arterivirus has a similar basic genome organization as MHV and also produces a 3′-coterminal nested set of sgRNAs. A mutation causing a twofold reduction in the amount of sgRNA3 of this virus resulted in a corresponding reduction in the amount of GP3 but in a fourfold reduction of the virus titer (Pasternak *et al.,* 2000). These results support the notion that corona- and related viruses (i.e., nidoviruses) have evolved to regulate, through the use of sgRNAs, the expression of their polycistronic genome, thus providing them with a mechanism to synthesize their proteins in optimal relative quantities.

In the past a number of coronaviruses have been described that carry mutations in or around one or more of their group-specific genes. While in some cases these mutations were demonstrated in viral genomes isolated directly from the animal, very often it is not clear whether they had been generated during passage of these viruses *in vitro*. Obviously, the generally high rate of mutation in RNA viruses and, in addition, the high frequency of homologous recombination of coronaviruses would be expected to lead to mutations that we now know not to hinder the replication capacity in cell culture. For example, an efficiently replicating MHV deletion mutant lacking a functional ns2 gene was obtained after extensive *in vitro* passaging of an MHV-JHM isolate (Schwarz *et al.,* 1990). The HE locus is highly heterogeneous among MHV strains (Luytjes, 1995; Yokomori *et al.,* 1991). While the gene is intact in strains JHM and S, MHV-A59 does not express its HE gene as it not only lacks the initiation codon but also a functional TRS (Luytjes *et al.,* 1988). A spectrum of 3′-truncated HE gene variants was observed in brains of mice inoculated with a MHV-JHM strain (Yokomori *et al.,* 1993). Similarly, considerable variation has also been found in the ORF 4 region of the group 2 coronaviruses. While a single ORF is located in MHV-JHM (Skinner and Siddell, 1985) and MHV-S (Yokomori and Lai, 1991), in MHV-A59 gene 4 is disrupted by a frameshift that results in two ORFs, 4a and 4b, of which only 4a is expressed (Weiss *et al.,* 1993). The MHV-A59 ORF4b is a shorter homolog of the MHV-JHM ORF4. In MHV-S the ORF4 is not expressed due to mutations in the TRS. The BCoV genome also contains two ORFs in this region, whereas in HCoV-OC43 a deletion has left only a small portion of the first ORF (Mounir and Talbot, 1993). Less heterogeneity has been observed for ORF5a, although a deletion in this region has been observed in MHV-S (Yokomori and Lai, 1991).

Deletion of the coronavirus group-specific genes in a controlled genetic background generated viruses that were attenuated in their natural host. The genetically minimized coronavirus was attenuated more severely than the other deletion mutant viruses. These observations suggest that the functional significance of the coronavirus group-specific genes relates to their role in vi-

rus–host interactions. Considering again these viruses' high frequency of mutation and recombination, these accessory genes would otherwise not have been maintained in the viral genome. However, although deletion of the MHV 2a/HE gene cluster did not affect replication *in vitro*, viruses lacking the 4/5a cluster replicated to a lesser extent. Therefore, while a functional role for the 2a/HE cluster *in vivo* seems plausible, the observed phenotypes of the viruses lacking the 4/5a cluster may well be caused by their reduced replication per se. Indeed, a recombinant MHV-JHM in which the gene 4 was genetically inactivated was not attenuated in a murine model of encephalitis (Ontiveros *et al.,* 2001). Consequently, as a next step to elucidate the significance of the MHV group-specific genes *in vivo*, these genes should be inactivated by site-specific mutagenesis.

Deletion of the coronavirus group-specific genes provides an attractive approach to generate attenuated live coronavirus vaccines. Analogous to MHV, the group-specific genes of other coronaviruses are anticipated to be accessory genes, the deletion of which is expected to result in attenuation without strongly affecting growth *in vitro*. In addition, creating genetically minimized coronaviruses may generate additional space for the stable insertion of foreign genes. The recent development of various reverse genetic procedures for coronaviruses will also enable the study of the other coronavirus group-specific genes and will finally pave the way for investigations into the pathogenesis of coronaviruses at the molecular level.

MATERIALS AND METHODS

Cells, viruses, and antibodies

MHV-A59 recombinants WT, Δ45a, Δ2aHE, and min were propagated in mouse LR7 cells (Kuo *et al.,* 2000), and plaque assays and plaque purifications were carried out with the same cells. Mouse 17 clone 1 (17Cl1) cells were used for radiolabeling of intracellular viral RNAs. Feline FCWF cells (American Type Culture Collection) were used for infection with the interspecies chimeric coronavirus virus fMHV (Kuo *et al.,* 2000). The rabbit polyclonal antiserum K134 to MHV-A59 (Rottier *et al.,* 1981), the antiserum UP3 to the 2a protein of MHV-A59 (Zoltick *et al.,* 1990), and the antiserum K5379 to the E protein of MHV-A59 (Raamsman *et al.,* 2000) have been described previously.

Plasmid constructs

Transcription vectors for the production of synthetic donor RNA for targeted recombination were derived from the plasmid pMH54 (Kuo *et al.*, 2000), which specifies a defective MHV-A59 RNA transcript consisting of the 5′ end of the genome (467 nt) fused to codon 28 of the HE gene and running to the 3′ end of the genome (Fig. 1). Plasmid pMH54 was used to construct a recombinant wild-type virus MHV-WT. Transcription vector pXHΔ45a lacks the ORFs 4a, 4b, and almost all of 5a. For the construction of this plasmid a PCR product was obtained from an MHV-A59-derived cDNA clone, pB59 (Fischer *et al.,* 1997), by using primer 1089 (5′-ACCTGCAGGACTAATCTAAACTTTATTCTTTTTAGGGCCACGC-3′), which contains a *Pst*I/*Sse*8387I restriction sequence and a TRS and which is complementary to the sequence just upstream of the E gene, and primer 1092 (5′-CCTTAAGGAATTGAACTGC-3′), which is complementary to the 5′ end of the M gene. The PCR product was cloned into pGEM-T Easy (Promega) according to the manufacturer's instructions, yielding pXH0803. The PCR product was subsequently excised with *Pst*I and *Eco*RV and cloned into *Sse*8387-I and *Eco*RV-treated pMH54, resulting in pXHΔ45a. Transcription vector pXHΔ2aHE lacks ORFs 2a and HE and contains approximately 1200 bp from the 3′ end of the replicase gene fused to the S gene. To construct this plasmid a PCR product was obtained by splicing overlap extension PCR. One PCR product was obtained from another MHV-A59 cDNA clone p96 (Bredenbeek *et al.,* 1990b) using primer 1128 (5′-ACGGTCCGACTGCGCGCTTGAACACGTTG-3′), which contains a *Rsr*II restriction sequence and is complementary to a region approximately 1200 bp upstream of the replicase stop codon, and primer 1130 (5′-CATGCAAGCTTTATTTGACATTTACTAGGCT-3′), which is complementary to the 3′ end of the replicase coding region and the TRS region that is located upstream of the S gene. The other PCR product was obtained from pMH54 using primer 1129 (5′-GTCAAATAAAGCTTGCATGAGGCATAATCTAAAC-3′), which is complementary to primer 1130, and primer 1127 (5′-CCAGTAAGCAATAATGTGG-3′), which is complementary to a region in the 5′ domain of the S gene. The PCR products were purified, mixed, and used in a PCR with primers 1128 and 1127. The DNA product obtained after the second round of PCR was cloned into pGEM-T Easy, yielding pXH1802. It was excised again with *Rsr*II and *Avr*II and cloned into pMH54, which had been treated with the same enzymes, resulting in pXHΔ2aHE. Transcription vector pXHmin contains the replicase 3′ end fused to the S gene and the deletion of ORFs 4a, 4b, and 5a. This vector was constructed by cloning the fragment excised with *Pst*I and *Eco*RV from pXH0803 into pXHΔ2aHE, which had been treated with *Sse*8387I and *Eco*RV. The composition of all PCR-generated segments was confirmed by DNA sequencing.

Construction of MHV mutants

Incorporation of mutations into the MHV genome by targeted RNA recombination was carried out as described previously (Hsue *et al.,* 2000). Donor RNAs transcribed from *Pac*I-truncated, pMH54-derived plasmids were transfected by electroporation into feline FCWF cells that had been infected 4 h earlier with fMHV (Kuo *et*

al., 2000). These cells were then plated onto a monolayer of mouse LR7 cells. After 24 h of incubation at 37°C, progeny viruses released into the cell culture media were harvested and candidate recombinants were selected by two rounds of plaque purification on LR7 cells. The mutations introduced into the viral genomes were confirmed by sequencing of RT-PCR products of the relevant regions prepared by using purified genomic RNA (Fig. 2), which were cloned into pGEM-T Easy. The primers used for the RT-PCR analysis were primer 1092, primer 990 (5′-CCTGATTTATCTCTC-GATTTC-3′), primer 1261 (5′-GCTGCTTACTCCTATCATAC-3′), primer 1127, primer 1173 (5′-GACTTAGTCCTCTCCT-TGA-3′), and primer 1260 (5′-CTTCAACGGTCTCAGTGC-3′) (Fig. 2).

Radiolabeling of viral RNA

The metabolic labeling of virus-specific RNAs was carried out essentially as reported previously (Masters *et al.,* 1994; Hsue and Masters, 1999). Briefly, 17Cl1 cell monolayers were infected with each MHV recombinant at a multiplicity of 5 PFU per cell. At 2 h postinfection, cells were starved for 4 h in Eagle's MEM containing 5% dialyzed fetal bovine serum (FBS) and 1/10 of the normal phosphate concentration. Cells were then labeled for 2 h with [^{33}P]orthophosphate in phosphate-free Eagle's MEM containing 5% dialyzed FBS and 20 μg actinomycin D (Sigma) per milliliter. Total cytoplasmic RNA was purified using Ultraspec reagent (Biotecx). Samples of RNA were denatured with formaldehyde and formamide, separated by electrophoresis through 1% agarose containing formaldehyde, and visualized by fluorography.

Metabolic labeling and immunoprecipitation

LR7 cells were grown and infected with each virus at a multiplicity of 8 PFU per cell. Before being labeled, cells were starved for 30 min in cysteine- and methionine-free minimal essential medium containing 10 mM HEPES (pH 7.2) and 5% dialyzed fetal bovine serum. The medium was then replaced by 600 μl of the same medium containing 100 μCi *in vitro* cell-labeling mix (Amersham). Cells were labeled from 5 to 8 h postinfection. At the end of the labeling period, culture media were collected, cleared by low-speed centrifugation, and prepared for immunoprecipitation by the addition of 1/4 vol of 5× concentrated lysis buffer (de Haan *et al.,* 1998). Proteins were immunoprecipitated from cell lysates as described before (de Haan *et al.,* 1998). Per immunoprecipitation 2.5 μl of anti-MHV, 3 μl of anti-E serum, and 3 μl of anti-2a serum were used. Immune complexes were adsorbed to Pansorbin cells (Calbiochem) for 30 min at 4°C and were subsequently collected by centrifugation. Pellets were washed four times by resuspension and centrifugation using wash buffers as described before (de Haan *et al.,* 1998). The final pellets were suspended in electrophoresis sample buffer. The immunoprecipitates were heated for 2 min at 95°C and analyzed by SDS–PAGE in 15% polyacrylamide gels.

One-step growth curve

LR7 cell monolayers were grown in 35-mm dishes in DMEM supplemented with 10% FBS. Confluent monolayers were infected in parallel with each virus (8 PFU/cell) and incubated for 1 h at 37°C. After absorption, the cells were washed with PBS three times and then fed with 2 ml of DMEM–10% FBS. Viral infectivity in culture media at different times postinfection was determined by a quantal assay on LR7 cells, and 50% tissue culture infective doses ($TCID_{50}$) were calculated.

Animals

C57Bl/6 (B6) mice were purchased from the National Cancer Institute (Frederick, MD). Four-week-old, MHV-free male mice were used in all experiments. Mice were anesthetized with isoflurane (IsoFlo; Abbott Laboratories, North Chicago, IL). The amount of virus designated in each experiment was diluted in PBS containing 0.75% bovine serum albumin, and a total volume of 20 μl was injected into the left cerebral hemisphere. Mock-infected controls were inoculated similarly.

Virulence assays

LD_{50} assays were carried out as described previously (Hingley *et al.,* 1994). Mice were inoculated intracranially with 5- or 10-fold serial dilutions of recombinant viruses. A total of five animals per dilution per virus were analyzed. Mice were examined for signs of disease or death on a daily basis up to 21 days postinfection. LD_{50} values were calculated by the Reed–Muench method (Reed and Muench, 1938).

ACKNOWLEDGMENTS

We gratefully acknowledge Su-hun Seo for excellent technical assistance with the virulence assays. We thank Lars de Haan for stimulating discussions. This work was carried out in part with financial support from the Commission of the European Communities, specific RTD programme "Quality of life and Management of Living Resources," QLK2-CT-1999-00002, "Generic coronavirus vaccine vectors for protection of farm animals against mucosal infections" to C.A.M.d.H. and P.J.M.R. This work does not necessarily reflect the Commission's views and in no way anticipates the Commission's future policy in this area. This work was also supported in part by Public Health Service Grant AI-45695 and AI-17418 from the National Institutes of Health to P.S.M. and S.W., respectively.

REFERENCES

Almazan, F., Gonzalez, J. M., Penzes, Z., Izeta, A., Calvo, E., Plana-Duran, J., and Enjuanes, L. (2000). Engineering the largest RNA virus ge-

nome as an infectious bacterial artificial chromosome. *Proc. Natl. Acad. Sci. USA* **97,** 5516–5521.

Bredenbeek, P. J., Noten, A. F., Horzinek, M. C., and Spaan, W. J. (1990). Identification and stability of a 30-kDa nonstructural protein encoded by mRNA 2 of mouse hepatitis virus in infected cells. *Virology* **175,** 303–306.

Bredenbeek, P. J., Pachuk, C. J., Noten, A. F., Charite, J., Luytjes, W., Weiss, S. R., and Spaan, W. J. (1990). The primary structure and expression of the second open reading frame of the polymerase gene of the coronavirus MHV-A59; a highly conserved polymerase is expressed by an efficient ribosomal frameshifting mechanism. *Nucleic Acids Res.* **18,**1825–1832.

Brian, D. A., Hogue, B. G., and Kienzle, T. E. (1995). The coronavirus hemagglutinin esterase glycoprotein. *In* "The Coronaviridae" (S. G. Siddell, Ed.), pp. 165–179. Plenum Press, New York.

Brown, T. D. K., and Brierly, I. (1995). The coronavirus nonstructural proteins. The coronavirus hemagglutinin esterase glycoprotein. *In* "The Coronaviridae" (S. G. Siddell, Ed.), pp. 191–217. Plenum Press, New York.

Chen, D., Luongo, C. L., Nibert, M. L., and Patton, J. T. (1999). Rotavirus open cores catalyze 5′-capping and methylation of exogenous RNA: Evidence that VP3 is a methyltransferase. *Virology* **265,** 120–130, doi:10.1006/viro.1999.0029.

Cox, G. J., Parker, M. D., and Babiuk, L. A. (1991). Bovine coronavirus nonstructural protein ns2 is a phosphoprotein. *Virology* **185,** 509–512.

de Haan, C. A. M., Kuo, L., Masters, P. S., Vennema, H., and Rottier, P. J. M. (1998). Coronavirus particle assembly: Primary structure requirements of the membrane protein. *J. Virol.* **72,** 6838–6850.

Ebner, D., Raabe, T., and Siddell, S. G. (1988). Identification of the coronavirus MHV-JHM mRNA 4 product. *J. Gen. Virol.* **69,** 1041–1050.

Emerman, M., and Malim, M. H. (1998). HIV-1 regulatory/accessory genes: Keys to unraveling viral and host cell biology. *Science* **280,** 1880–1884.

Fischer, F., Stegen, C. F., Koetzner, C. A., and Masters, P. S. (1997). Analysis of a recombinant mouse hepatitis virus expressing a foreign gene reveals a novel aspect of coronavirus transcription. *J. Virol.* **71,** 5148–5160.

Fischer, F., Stegen, C. F., Masters, P. S., and Samsonoff, W. A. (1998). Analysis of constructed E gene mutants of mouse hepatitis virus confirms a pivotal role for E protein in coronavirus assembly. *J. Virol.* **72,** 7885–7894.

Hingley, S. T., Gombold, J. L., Lavi, E., and Weiss, S. R. (1994). MHV-A59 fusion mutants are attenuated and display altered hepatotropism. *Virology* **200,** 1–10, doi:10.1006/viro.1994.1156.

Hsue, B., Hartshorne, T., and Masters, P. S. (2000). Characterization of an essential RNA secondary structure in the 3′ untranslated region of the murine coronavirus genome. *J. Virol.* **74,** 6911–6921.

Hsue, B., and Masters, P. S. (1999). Insertion of a new transcriptional unit into the genome of mouse hepatitis virus. *J. Virol.* **73,** 6128–6135.

Jacobs, L., Spaan, W. J., Horzinek, M. C., and van der Zeijst, B. A.. (1981). Synthesis of subgenomic mRNA's of mouse hepatitis virus is initiated independently: Evidence from UV transcription mapping. *J. Virol.* **39,** 401–406.

Jendrach, M., Thiel, V., and Siddell, S. G. (1999). Characterization of an internal ribosome entry site within mRNA 5 of murine hepatitis virus. *Arch. Virol.* **144,** 921–933.

Krijnse Locker, J., Griffiths, G., Horzinek, M. C., and Rottier, P. J. M. (1992). O-glycosylation of the coronavirus M protein. Differential localization of sialyltransferases in N- and O-linked glycosylation. *J. Biol. Chem.* **267,** 14094–14101.

Kuo, L., Godeke, G. J., Raamsman, M. J., Masters, P. S., and Rottier, P. J. M. (2000). Retargeting of coronavirus by substitution of the spike glycoprotein ectodomain: Crossing the host cell species barrier. *J. Virol.* **74,** 1393–1406.

Labonte, P., Mounir, S., and Talbot, P. J. (1995). Sequence and expression of the ns2 protein gene of human coronavirus OC43. *J. Gen. Virol.* **76,** 431–435.

Lai, M. M., and Cavanagh, D. (1997). The molecular biology of coronaviruses. *Adv. Virus Res.* **48,**1–100.

Leibowitz, J. L., Wilhelmsen, K. C., and Bond, C. W. (1981). The virus-specific intracellular RNA species of two murine coronaviruses: MHV-A59 and MHV-JHM. *Virology* **114,** 39–51.

Luytjes, W. (1995). Coronavirus gene expression. *In* "The Coronaviridae" (S. G. Siddell, Ed.), pp. 33–54. Plenum Press, New York.

Luytjes, W., Bredenbeek, P. J., Noten, A. F., Horzinek, M. C., and Spaan, W. J. (1988). Sequence of mouse hepatitis virus A59 mRNA 2: Indications for RNA recombination between coronaviruses and influenza C virus. *Virology* **166,** 415–422.

Masters, P. S. (1999). Reverse genetics of the largest RNA viruses. *Adv. Virus Res.* **53,** 245–264.

Masters, P. S., Koetzner, C. A., Kerr, C. A., and Heo, Y. (1994). Optimization of targeted RNA recombination and mapping of a novel nucleocapsid gene mutation in the coronavirus mouse hepatitis virus. *J. Virol.* **68,** 328–337.

Mounir, S., and Talbot, P. J. (1993). Human coronavirus OC43 RNA 4 lacks two open reading frames located downstream of the S gene of bovine coronavirus. *Virology* **192,** 355–360, doi:10.1006/viro.1993.1043.

Ontiveros, E., L. Kuo, P. S. Masters, and S. Perlman. (2001). Inactivation of expression of gene 4 of mouse hepatitis virus strain JHM does not affect virulence in the murine CNS. *Virology* **289,** 230–238, doi: 10.1006/viro.2001.1167.

Opstelten, D.-J. E. (1995). "Envelope Glycoprotein Interaction in Coronavirus Assembly." Ph.D. Thesis, Utrecht University, The Netherlands.

Pasternak, A. O., Gultyaev, A. P., Spaan, W. J., and Snijder, E. J. (2000). Genetic manipulation of arterivirus alternative mRNA leader-body junction sites reveals tight regulation of structural protein expression. *J. Virol.* **74,** 11642–11653.

Ploegh, H. L. (1998). Viral strategies of immune evasion. *Science* **280,** 248–253.

Raamsman, M. J., Krijnse Locker, J., de Hooge, A., de Vries, A. A., Griffiths, G., Vennema, H., and Rottier, P. J. M. (2000). Characterization of the coronavirus mouse hepatitis virus strain A59 small membrane protein E. *J. Virol.* **74,** 2333–2342.

Reed, L. J., and Muench, H. (1938). A simple method of estimating fifty percent points. *Am. J. Hyg.* **27,** 493–497.

Rottier, P. J. M., Horzinek, M. C., and van der Zeijst, B. A. (1981). Viral protein synthesis in mouse hepatitis virus strain A59-infected cells: Effect of tunicamycin. *J. Virol.* **40,** 350–357.

Sawicki, S. G., and Sawicki, D. L. (1998). A new model for coronavirus transcription. *Adv. Exp. Med. Biol.* **440,** 215–219.

Schwarz, B., Routledge, E., and Siddell, S. G. (1990). Murine coronavirus nonstructural protein ns2 is not essential for virus replication in transformed cells. *J. Virol.* **64,** 4784–4791.

Skinner, M. A., and Siddell, S. G. (1985). Coding sequence of coronavirus MHV-JHM mRNA 4. *J. Gen. Virol.* **66,** 593–596.

Snijder, E. J., den Boon, J. A., Horzinek, M. C., and Spaan, W. J. (1991). Comparison of the genome organization of toro- and coronaviruses: Evidence for two nonhomologous RNA recombination events during Berne virus evolution. *Virology* **180,** 448–452.

Thiel, V., Herold, J., Schelle, B., and Siddell, S. G. (2001). Infectious RNA transcribed in vitro from a cDNA copy of the human coronavirus genome cloned in vaccinia virus. *J. Gen. Virol.* **82,** 1273–1281.

Vennema, H., Godeke, G. J., Rossen, J. W., Voorhout, W. F., Horzinek, M.C, Opstelten, D. J., and Rottier, P. J. M. (1996). Nucleocapsid-independent assembly of coronavirus-like particles by co-expression of viral envelope protein genes. *EMBO J.* **15,** 2020–2028.

Weiss, S. R., Zoltick, P. W., and Leibowitz, J. L. (1993). The ns 4 gene of mouse hepatitis virus (MHV), strain A 59 contains two ORFs and thus differs from ns 4 of the JHM and S strains. *Arch. Virol.* **129,** 301–309.

Yokomori, K., Banner, L. R., and Lai, M. M. (1991). Heterogeneity of gene expression of the hemagglutinin-esterase (HE) protein of murine coronaviruses. *Virology* **183,** 647–657.

Yokomori, K., and Lai, M. M. (1991). Mouse hepatitis virus S RNA sequence reveals that nonstructural proteins ns4 and ns5a are not essential for murine coronavirus replication. *J. Virol.* **65,** 5605–5608.

Yokomori, K., Stohlman, S. A., and Lai, M. M. (1993). The detection and characterization of multiple hemagglutinin-esterase (HE)-defective viruses in the mouse brain during subacute demyelination induced by mouse hepatitis virus. *Virology* **192,** 170–178, doi:10.1006/viro.1993.1019

Yount, B., Curtis, K. M., and Baric, R. S. (2000). Strategy for systematic assembly of large RNA and DNA genomes: Transmissible gastroenteritis virus model. *J. Virol.* **74,** 10600–10611.

Zoltick, P. W., Leibowitz, J. L., Oleszak, E. L., and Weiss, S. R. (1990). Mouse hepatitis virus ORF 2a is expressed in the cytosol of infected mouse fibroblasts. *Virology* **174,** 605–607.